

ON THE WELDED TUBE MAP

BENJAMIN AUDOUX

ABSTRACT. This paper investigates the so-called Tube map which connects welded knots, that is a quotient of the virtual knot theory, to ribbon torus-knots, that is a restricted notion of fillable knotted tori in S^4 . It emphasizes the fact that ribbon torus-knots with a given filling are in one-to-one correspondence with welded knots before quotient under classical Reidemeister moves and reformulates these moves and the known source of non-injectivity of the Tube map in terms of filling changes.

This papers investigates a known connection between two notions of distinct nature : welded knots, which are combinatorial elements of a quotient of the virtual knot theory; and ribbon torus-knots, which are a restricted notion of topological knotted surfaces in S^4 .

Virtual knots are a completion of usual knots, seen from the diagrammatical point of view. Knot diagrams can be thought of as abstract oriented circles with a pairing, that is a finite number of signed pairs of ordered “merged” points. Indeed, as shown in Figure 1, every such ordered and signed pair describes a crossing and the rest of the circle prescribes how the ends of these crossings are connected; up to isotopy, this data is sufficient to recover a diagram and hence a knot in \mathbb{R}^3 . However, not all pairings are realizable as a diagram since it may be impossible to connect, in the plane, all ends as prescribed without introducing some additional crossing. A virtual knot is such an abstract circle with a pairing, whether it is realizable or not, up to some relevant moves inherited from the usual knot theory. Equivalently, it can be described as a diagram with possibly some additional *virtual* crossings, represented as circled crossings, which are not reported in the pairing.

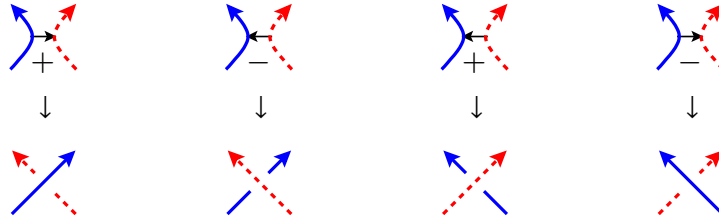


FIGURE 1. Correspondance between oriented and signed pairs and crossings

Virtual knots can be interpreted as knots in thickened surfaces modulo handle stabilization [CKS02, Kup03]. Because of the stabilizations, this does not provide a well defined notion of complement; in spite of that, the usual notion of knot group, *i.e.* fundamental group of the complement, can be combinatorially extended to the virtual case [Kim00, SW00, BB14]. Knot groups happens to be invariant under the so-called *over-commute move* (OC), a move (see Figure 7) which, in general, modifies virtual knots. There are other topological invariants which, similarly, can be combinatorially extended and proved to be invariant under OC. This motivates the definition of *welded knots* which are the quotient of virtual knots under these moves. Welded knotted objects first appeared in a work of Fenn-Rimanyi-Rourke in the more algebraic context of braids [FRR97]. At this stage, one can hope that welded knots admit a deeper topological interpretation

Date: August 7, 2015.

2010 Mathematics Subject Classification. 57Q45.

Key words and phrases. ribbon singularities, ribbon (solid) torus, ribbon torus-knots, welded diagrams, welded knots, Tube map.

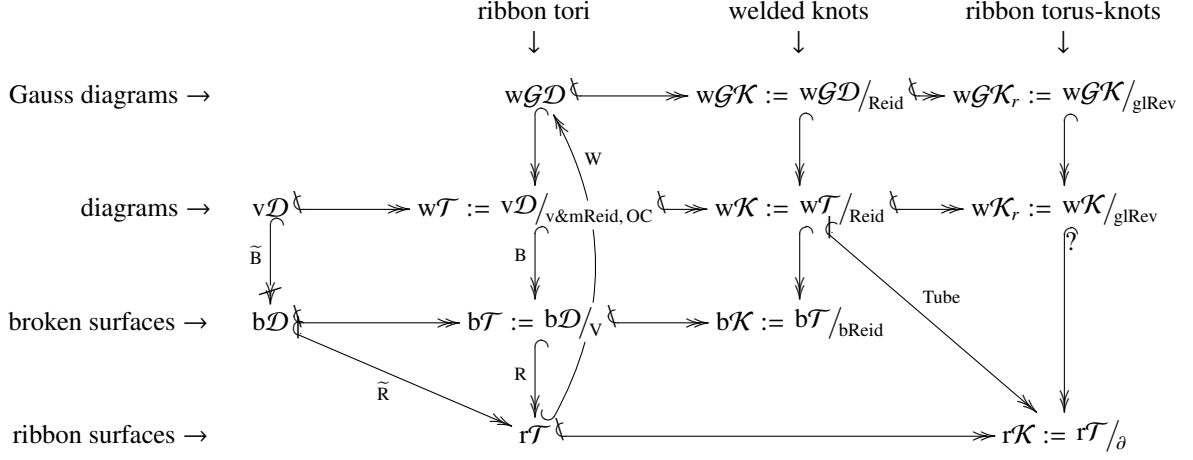


FIGURE 2. Summary of the combinatorial and/or topological sets and their connections

than virtual knots do, yielding back a topological nature for the combinatorial extension of the invariants mentioned above.

The theory of knotted surfaces in 4-space takes its origins in the mid-twenties from the work of Artin [Art25]. However, the systematic study of these objects only really began in the early sixties, notably through the work of Kervaire, Fox and Milnor [KM61, Ker65, FM66], but also in a series of papers from Kansai area, Japan (see references in [Suz76]). From this early stage, the class of ribbon surfaces was given a particular attention. Roughly speaking, an embedded surface in S^4 is ribbon if it can be filled by an immersed 3-manifold whose singular set is a finite number of rather simple singularities called *ribbon disks*. Asking for the surface to be fillable does not change the notion of isotopy but restrict the equivalence classes we are looking at. Indeed, an ambient isotopy transport as well any given filling, so two isotopic surfaces are simultaneously fillable or not. On the contrary, asking for a surface to be actually filled multiplies the number of equivalence classes since a single surface may have several non isotopic fillings. Asking for filledness better than for fillability is hence more constraining but — at least, this is what the present paper tends to show — it is easier to handle. Fillable surfaces are furthermore obtained as the quotient of filled surfaces under filling changes.

The case of the torus was already addressed in [Yaj62] under the name of ribbon torus-knots. In his paper, T. Yajima laid the foundation of the so-called Tube map which inflates usual knot into ribbon torus-knots. In [Sat00], S. Satoh shows that this map can actually be extended to all welded knots. He proves moreover that the map is then surjective, that the welded combinatorial knot group corresponds to the fundamental group of the complement in S^4 of the image, and that it commutes with the orientation reversals — what is not direct from the definition but a consequence of the torus eversion in S^4 . Ribbon torus-knots are hence good candidates for a topological interpretation of welded knots. However the Tube map is not injective and the lack of injectivity is not fully understood yet: the Tube map is known to be invariant under a global reversal move (see Prop. 3.4 in [IK12] or Prop. 2.7 in the present paper) but it is not known whether the Tube map quotiented by this move is injective.

This paper contains no new result, but it reviews and reformulates the construction of the Tube map. In particular, it emphasizes the fact that ribbon torus-knot with a given filling are in one-to-one correspondence with welded knots before quotient under classical Reidemeister moves. We interpret then invariance of the Tube map under Reidemeister moves, and notably Reidemeister move I which is the most intricate one, in terms of local filling changes. The global reversal move which let the Tube map invariant is also interpreted as a co-orientation change in the filling. Another goal of this paper is to clarify the relationship between three kind of objects:

- ribbon ones which are 2 or 3-dimensional objects inside a 4-dimensional space;

- broken ones, which are decorated 2–dimensional objects inside a 3–dimensional space;
- welded ones which are decorated 1–dimensional objects inside a 2–dimensional space. There is also one exceptional item, namely welded Gauss diagrams, which is purely combinatorial.

They are, respectively, denoted with a small “r”, “b” or “w” prefix.

The paper is organized as follows. The first section defines all the topological and/or combinatorial notions of knotted objects. There is a lot of redundancy in these notions; a summary of them is given in Figure 2. In the second section, all maps between the different notions are defined, in particular the Tube map. The non-injectivity is discussed there. The last section addresses the notion of *wen*, which is a special portion of ribbon torus-knot embedded in S^4 as a Klein bottle cut along a meridional circle. *Wens* shall appear as items we want to avoid when projecting ribbon torus-knots in S^3 , but also as a useful tool for addressing Reidemeister move I and the commutation of the Tube map with the orientation reversals.

Acknowledgments. This paper was initiated after a talk of the author at the conference “Advanced school and discussion meeting on Knot theory and its applications”, organized at IISER Mohali in december 2013. The author is grateful to Krishnendu Gongopadhyay for inviting him. He also warmly thanks Ester Dalvit, Paolo Bellingeri, Jean-Baptiste Meilhan and Emmanuel Wagner for encouraging and stimulating conversations, and Hans Boden for pointing out a mistake in a previous version. This work is supported by the French ANR research project “VasKho” ANR-11-JS01-00201.

1. RIBBON, BROKEN AND WELDED OBJECTS

1.1. Ribbon tori and ribbon torus-knots. By convention, an immersion shall actually refer to the image $\text{Im}(\tilde{Y} \hookrightarrow X) \subset X$ of the immersion, whereas the immersed space \tilde{Y} shall be referred to as the associated *abstract space*. Throughout this paper, every immersion $Y \subset X$ shall be considered *locally flat*, that is locally homeomorphic to a linear subspace \mathbb{R}^k in \mathbb{R}^m for some positive integers $k \leq m$, except on ∂Y (resp. ∂X), where \mathbb{R}^k (resp. \mathbb{R}^m) should be replaced by $\mathbb{R}_+ \times \mathbb{R}^{k-1}$ (resp. $\mathbb{R}_+ \times \mathbb{R}^{m-1}$); and every intersection $Y_1 \cap Y_2 \subset X$ shall be considered *flatly transverse*, that is locally homeomorphic to the intersection of two linear subspaces \mathbb{R}^{k_1} and \mathbb{R}^{k_2} in \mathbb{R}^m for some positive integers $k_1, k_2 \leq m$, except on ∂Y_1 (resp. ∂Y_2 , ∂X), where \mathbb{R}^{k_1} (resp. \mathbb{R}^{k_2} , \mathbb{R}^m) should be replaced by $\mathbb{R}_+ \times \mathbb{R}^{k_1-1}$ (resp. $\mathbb{R}_+ \times \mathbb{R}^{k_2-1}$, $\mathbb{R}_+ \times \mathbb{R}^{m-1}$).

Here, we shall consider 3–dimensional spaces immersed in S^4 in a quite restrictive way, since we allow only the following type of singularity.

Definition 1.1. An intersection $D := Y_1 \cap Y_2 \subset S^4$ is a *ribbon disk* if it is isomorphic to the 2–dimensional disk and satisfies $D \subset \mathring{Y}_1$, $\mathring{D} \subset \mathring{Y}_2$ and ∂D is an essential curve in ∂Y_2 .

Before defining the main topological objects of this paper, we want to stress the fact that, besides a 3–dimensional orientation, a solid torus can be given a co-orientation, that is a 1–dimensional orientation of its core. Note that orientation and co-orientation are independent notions and that the 3–dimensional orientation can be equivalently given as a 2–dimensional orientation on the boundary. We say that a solid torus is *bi-oriented* if it is given an orientation and a co-orientation.

Definition 1.2. A *ribbon torus* is a bi-oriented immersed solid torus $D^2 \times S^1 \subset S^4$ whose singular set consists of a finite number of ribbon disks.

We define $\text{r}\mathcal{T}$ as the set of ribbon tori up to ambient isotopy.

Definition 1.3. A *ribbon torus-knot* is an embedded oriented torus $S^1 \times S^1 \subset S^4$ which bounds a ribbon torus. We say that it admits a *ribbon filling*.

We define $\text{r}\mathcal{K}$ as the set of ribbon torus-knots up to ambient isotopy.

Definitions 1.2 and 1.3 use the same notion of ambient isotopy. By forgetting its interior and keeping only its boundary, one sends hence any ribbon torus to a ribbon torus-knot. However, a given ribbon torus-knot may have several non isotopic ribbon filling. It follows that $\text{r}\mathcal{K}$ may be seen as the non trivial quotient $\text{r}\mathcal{T}/\partial$, where ∂ is the equivalence relation generated by $T \stackrel{\partial}{\sim} T' \Leftrightarrow \partial T = \partial T'$.

Remark 1.4. To emphasize the connection with welded diagrams, we have chosen to deal with ribbon torus-knots, but other ribbon knotted objects in 4–dimensional spaces can be defined similarly, such as ribbon 2–knots [Yaj64, Yan69, Suz76, Coc83, KS02], ribbon 2–links, ribbon torus-links or ribbon tubes [ABMW14].

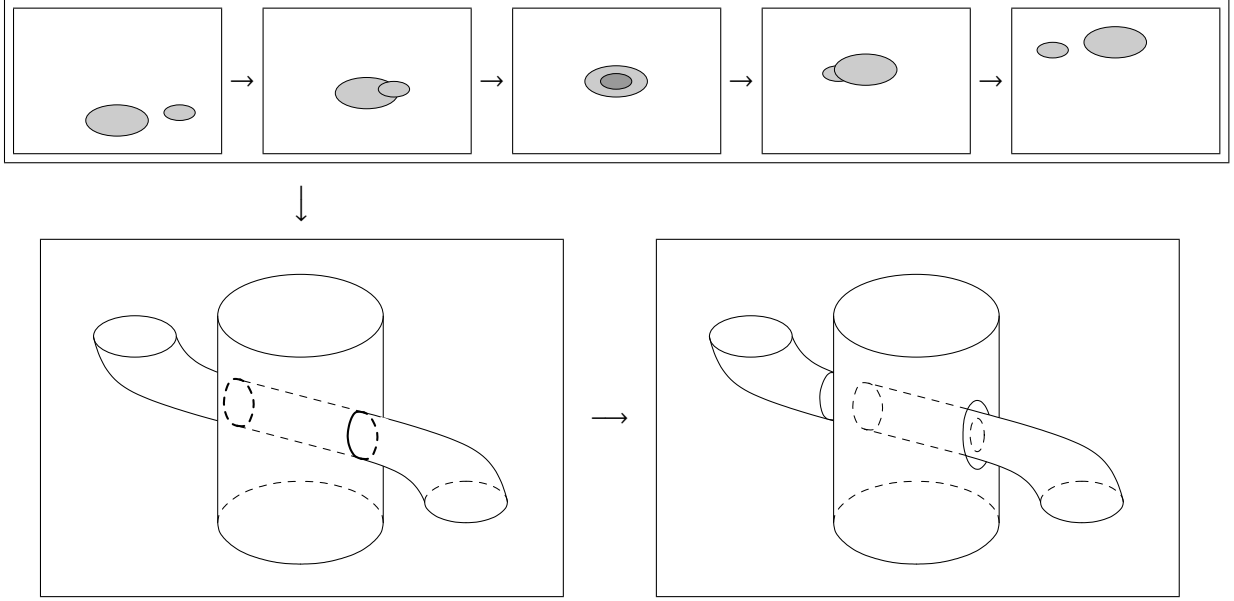
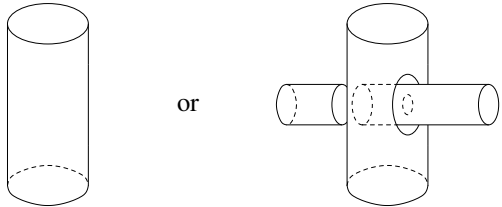


FIGURE 3. Around a ribbon disk

Since our considerations shall be local, most of the material in this paper can be transposed to any of these notions.

1.2. Broken torus diagrams. Away from ribbon disks, pieces of a ribbon torus-knot are just annuli which can be properly projected into tubes in \mathbb{R}^3 . Around any ribbon disk, the local flatness assumption allows a local parametrization as $B^3 \times [0, 1]$, where the last summand is seen as a time parameter so that the ribbon torus-knot locally corresponds to the motion of two horizontal circles, one flying through the other. Note that these flying circles arise naturally as the boundary of flying disks in \mathbb{R}^3 . By projecting along the time parameter, that is by keeping the residual track of the flying disks, we obtain two tubes, one passing through the other. In doing so, it creates two singular circles. But the tubes do not cross in S^4 so it means that for each singular circle, the time parameter separates the two preimages. There are hence one circle preimage on each tube, one having time parameters smaller than the other. By convention, we erase from the picture a small neighborhood of the preimage with the lowest projecting parameter. See Figure 3 for a picture. As we shall see, these local projections can actually be made global, and they motivate the following definition.

Definition 1.5. A *broken torus diagram* is a torus immersed in \mathbb{R}^3 whose singular set is a finite number of transverse singular circles, each of which is equipped with an order on its two preimages. As noted above and by convention, this order is specified on picture by erasing a small neighborhood of the lowest preimage. The broken surface diagram is furthermore said *symmetric* if it is locally homeomorphic to either



This means singular circles are pairwise matched in such a way that, for any pair, both circle has

- an essential preimage: they are consecutive on a tube and the piece of tube in-between is empty of any other singular circle;

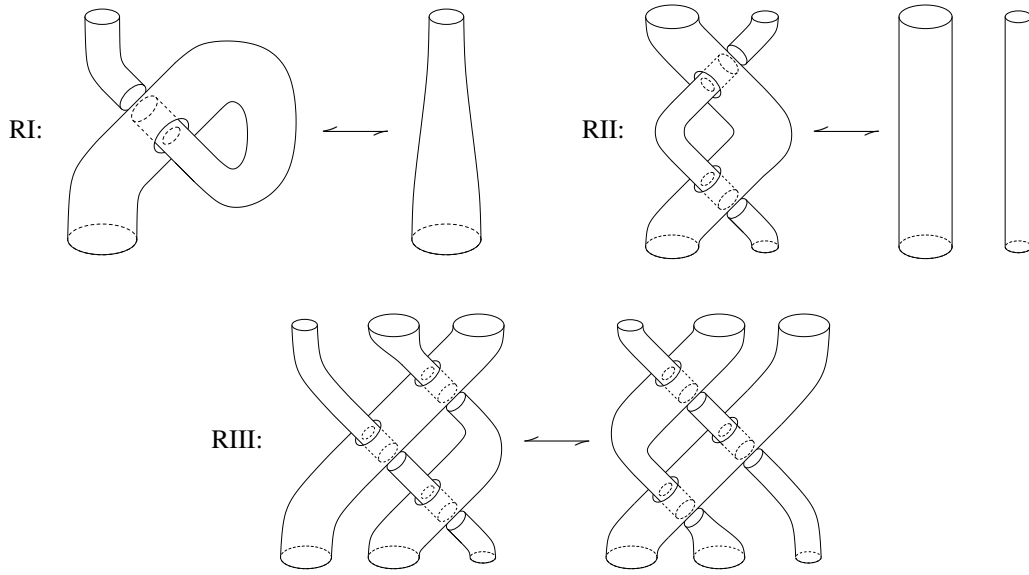


FIGURE 4. Broken Reidemeister moves bReid for broken torus diagrams:

in these pictures, each singularity of type can be turned into a type one;
 however, the two singularities of move RII and the two singularities on the widest tube of move RIII
 must be then turned simultaneously

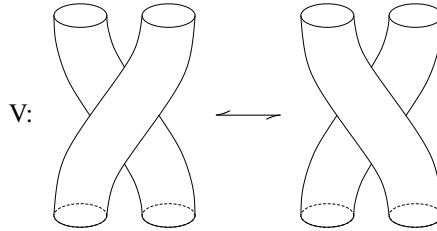


FIGURE 5. Virtual move for broken torus diagrams

- a non essential preimage: they are in the same connected component of the torus minus all essential preimages, and they are respectively higher and lower than their essential counterparts for the associated orders.

As is clear from the pictures above, a symmetric broken torus diagram comes with an obvious solid torus filling which is naturally oriented by the ambient space. It is hence sufficient to enhance it with a co-orientation to provide a bi-orientation. As a consequence, a symmetric broken torus diagram is said *bi-oriented* if its natural filling is given a co-orientation.

We define \mathbf{bD} the set of bi-oriented symmetric broken torus diagrams up to ambient isotopy. Unless otherwise specified, we shall assume, in the following, that all broken torus diagrams are symmetric.

A *local move* is a transformation that changes a diagrammatical and/or topological object only inside a ball of the appropriate dimension. By convention, we represent only the ball where the move occurs, and the reader should keep in mind that there is a non represented part, which is identical for each side of the move. Broken torus diagrams are higher-dimensional counterpart of usual knot diagrams. As such, we shall quotient them by some local moves.

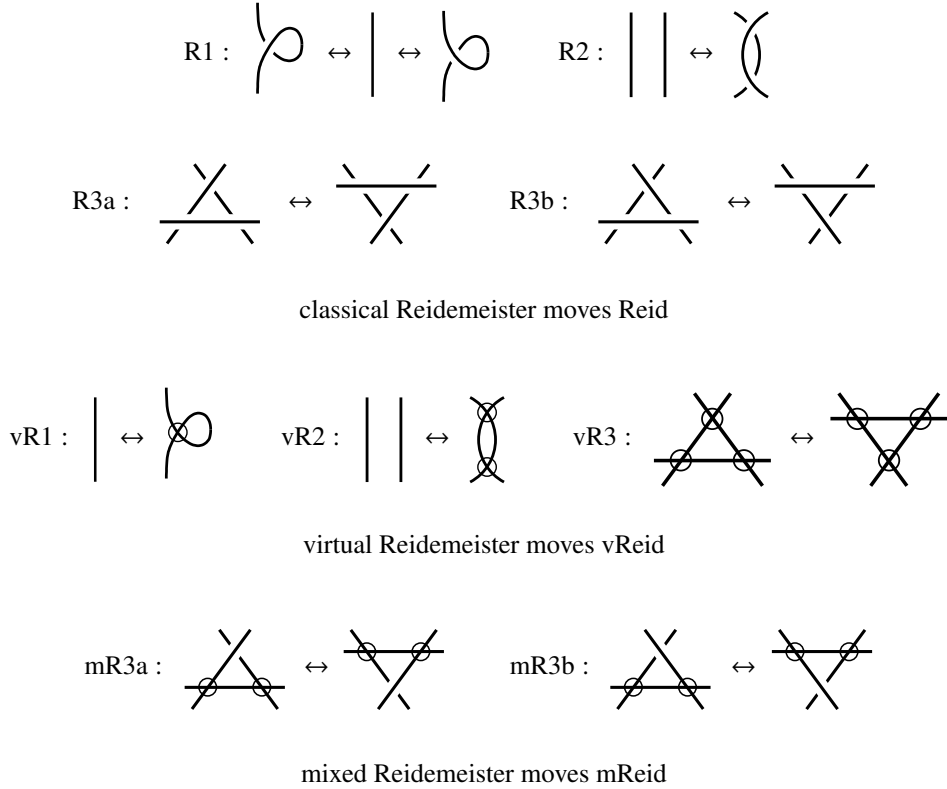


FIGURE 6. Generalized Reidemeister moves gReid on virtual diagrams

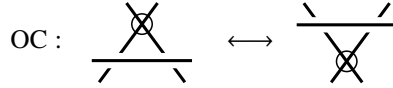


FIGURE 7. Over commute move on virtual diagrams

Definition 1.6. We define $b\text{Reid}$, the *broken Reidemeister moves*, and V , the *virtual move*, on broken torus diagrams as the local moves shown, respectively, in Figure 4 and 5. Moreover, we define the set $b\mathcal{T} := b\mathcal{D}/V$ of *broken tori* as the quotient of broken torus diagrams under the virtual move; and the set $b\mathcal{K} := b\mathcal{D}/b\text{Reid}, V$ of *broken knots* as the quotient of broken torus diagrams under virtual and broken Reidemeister moves, or equivalently as the quotient of broken tori under broken Reidemeister moves.

1.3. Welded knots. Broken torus diagrams appeared as a partially combinatorial “2 ↔ 3”-dimensional description of ribbon objects; but, as we shall see, this description can be cut down one dimension more.

Definition 1.7. A *virtual diagram* is an oriented circle immersed in \mathbb{R}^2 whose singular set is a finite number of transverse double points, called *crossing*, each of which is equipped with a partial order on its two preimages. By convention, this order is specified by erasing a small neighborhood of the lowest preimage, or by circling the crossing if the preimages are not comparable.

If the preimages of a crossing are comparable, then the crossing is said *classical*; otherwise it is said *virtual*. Moreover, a classical crossing is said *positive* if the basis made of the tangent vectors of the highest and lowest preimages is positive; otherwise, it is said *negative*.

We define $v\mathcal{D}$ as the set of virtual diagrams up to ambient isotopy.

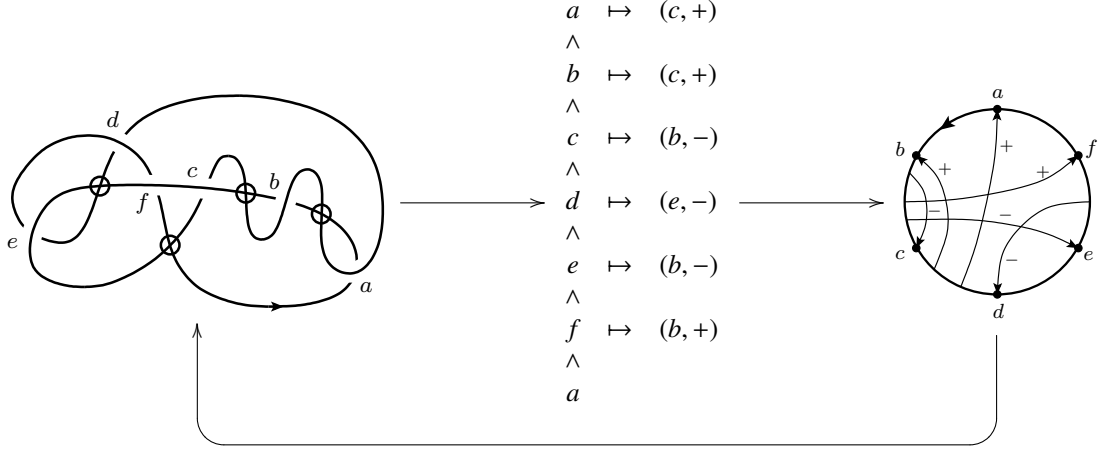


FIGURE 8. Diagrams, welded Gauss diagrams and Gauss diagrams

Definition 1.8. We define the *generalized Reidemeister moves* gReid — separated into classical moves Reid , virtual moves vReid and mixed moves mReid — and the *over commute move* OC on virtual diagrams as the local moves shown, respectively, in Figure 6 and 7. Moreover, we define the set $\text{w}\mathcal{T} := \text{v}\mathcal{D}/\text{vReid}, \text{mReid}, \text{OC}$ of *welded tori* as the quotient of virtual diagrams under virtual Reidemeister, mixed Reidemeister and over commute moves; and the set $\text{w}\mathcal{K} := \text{v}\mathcal{D}/\text{gReid}, \text{OC}$ of *welded knots* as the quotient of virtual diagrams under generalized Reidemeister and over commute moves, that is as the quotient of welded tori under classical Reidemeister moves.

Classical Reidemeister moves are vestiges of the diagrammatical description of the usual knot theory. Virtual and mixed Reidemeister moves essentially states that only classical crossings and the abstract connections between their endpoints are meaningful, and not the actual strands which realize these connections. Over commute move states that two classical crossings connected by a strand which is the highest strand for both crossing can be commuted. As a matter of fact, it only matters the cyclic order of lowest preimages of classical crossings, as they are met while running positively along the immersed oriented circle, and the unordered sets of highest preimages which are located between two consecutive lowest preimages. This motivates the following definition:

Definition 1.9. A welded Gauss diagram is a finite set C given with a cyclic order and a map from C to $C \times \{\pm 1\}$.

We define $\text{w}\mathcal{GD}$ the set of welded Gauss diagram.

Proposition 1.10. *There is a one-to-one correspondence between $\text{w}\mathcal{GD}$ and $\text{w}\mathcal{T}$.*

Proof. To a virtual diagram D , we associate a welded Gauss diagram as follows. When running along D , every crossing is met twice, once on the highest strand and once on the lowest one. So first, we consider C , the set of classical crossing of D , ordered by the order in which the crossings are met on the lowest strand while running positively along D . Then, to $c \in C$, we associate the sign of c and the last crossing met on the lowest strand, while running positively along D , before meeting c on the highest strand.

It is straightforwardly checked that this is invariant under virtual Reidemeister, mixed Reidemeister and over commute moves and that it defines a one-to-one map from $\text{w}\mathcal{T}$ to $\text{w}\mathcal{GD}$. This last statement can be verified by hand or, for readers who know about usual Gauss diagrams, by defining an inverse map, using item (2) in Remark 1.11 and the fact that Gauss diagrams up to tail commute moves are in one-to-one correspondence with welded diagrams. See Figure 8 for an illustration. \square

Remarks 1.11.

- (1) It is quite straightforward to define relevant moves on welded Gauss diagrams, denoted eponymously by Reid in Figure 2, that correspond to classical Reidemeister moves. The quotient is

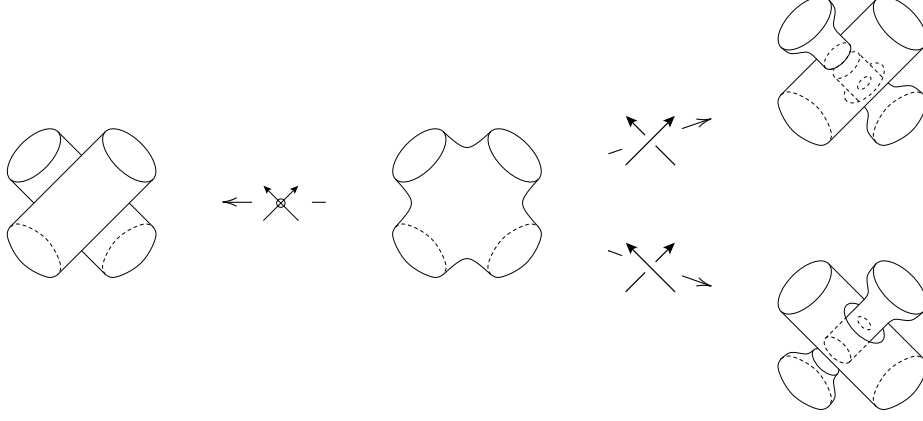


FIGURE 9. Inflating classical and virtual crossings

one-to-one with $w\mathcal{K}$, but since we shall not need them in this paper, we refer the interested reader to [ABMW14, Section 4.1] for a formal definition.

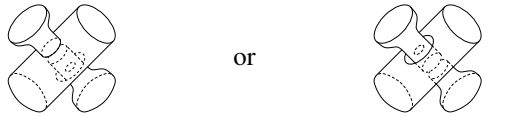
- (2) To a welded Gauss diagram $G : C \rightarrow C \times \{\pm 1\}$, one can associate a more traditional Gauss diagram (see [PV94, GPV00, Fie01, BND14a] for definitions and Figure 8 for an illustration) by
- using the cyclic order on C to mark one point for each element in C on an ordered circle;
 - between the point marked by $c \in C$ and its direct successor on the oriented circle, marking one more point for each preimage in $G^{-1}(c, \pm 1)$, no matter in which order;
 - for every $c \in C$, drawing arrows from the point marked by c' to the point marked by c with sign ε where $(c', \varepsilon) = G(c)$.

2. THE TUBE MAP

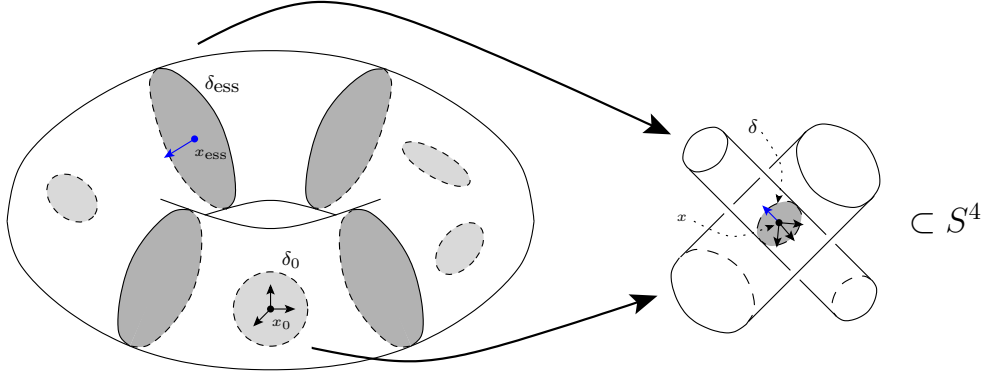
In this section, we define some maps between ribbon and welded objects. Broken objects shall appear as an in-between.

First, we define $\tilde{B} : v\mathcal{D} \rightarrow b\mathcal{D}$ as follows. Let D be a virtual diagram and consider it as a singular circle lying in $\mathbb{R}^2 \times \{0\} \subset \mathbb{R}^3$. Now, consider the boundary of a neighborhood of it in \mathbb{R}^3 . This is an handlebody whose boundary is the union of 4-punctured spheres, one for each crossing, attached along their boundaries. Every such punctured sphere is hence decorated by a partial order. We define $\tilde{B}(D)$ to be the broken torus diagram obtained by modifying locally each punctured sphere according to its partial order as shown in Figure 9. It is oriented by the ambient orientation of \mathbb{R}^3 and co-oriented by the orientation of D .

Remark 2.1. The piece of broken torus diagram associated to a classical crossing does not depend only on the crossing sign but also on the actual orientation. Indeed, reversing the orientation preserves signs but flips upside down Figure 9. For instance, depending on the orientation, a positive crossing can be sent to



which are not isotopic when fixing the boundaries. In particular, reversing the orientation of a diagram does not just reverse, in general, the co-orientation of the associated broken torus diagram. To realize such an

FIGURE 10. A picture for \tilde{T}

operation, the orientation should be reversed, but some virtual crossings should also be added before and after the crossing, and the sign of the crossing should moreover be switched. As a matter of fact, \times and \bowtie are sent to similar pieces of broken torus diagram with opposite co-orientations. This observation shall also follow from the behavior of the map W defined below under the co-orientation reversal.

Now, we define $\tilde{R} : b\mathcal{D} \rightarrow r\mathcal{T}$ as follows. Let T be a broken torus diagram and consider it as lying in $\mathbb{R}^3 \times \{0\} \subset S^4$. Then, near each singular circle, the thinnest tube can be pushed slightly above or below in the fourth dimension, depending on the order associated to this singular circle. The torus is then embedded in S^4 . But a symmetric broken torus diagram comes naturally with a filling by a solid torus and the pushing can be performed so that every pair of associated singular circles leads to a single ribbon disk singularity. We define $\tilde{R}(T)$ to be this immersed solid torus with the bi-orientation induced by the one of T .

Lemma 2.2. *The maps \tilde{B} and \tilde{R} descend to well-defined maps $B : w\mathcal{T} \rightarrow b\mathcal{T}$ and $R : b\mathcal{T} \rightarrow r\mathcal{T}$.*

Proof. To prove the statement on \tilde{R} , it is sufficient to prove that two broken torus diagrams which differ from a virtual move have the same image by \tilde{R} . Figure 13 gives an explicit isotopy showing that. Another projection of this isotopy can found at [Dal14]

Concerning \tilde{B} , it sends both sides of moves vR1 and OC on broken torus diagrams which are easily seen to be isotopic. For any of the other virtual and mixed Reidemeister moves, some preliminary virtual moves may be needed before the broken torus diagrams become isotopic. For instance, among the represented strands, one can choose one with two virtual crossings on it and, up to the virtual move, pull out its image by \tilde{B} in front of the rest; then both sides of the move are sent to isotopic broken torus diagrams. \square

Notation 2.3. We denote by $T : w\mathcal{T} \rightarrow r\mathcal{T}$ the composite map $R \circ B$.

The map T is actually a bijection. To prove this, we introduce $W : r\mathcal{T} \rightarrow w\mathcal{GD} \cong w\mathcal{T}$ defined as follows. Let T be a ribbon torus and \tilde{T} its abstract solid torus. We denote by C the set of ribbon disks of T . Each $\delta \in C$ has two preimages in \tilde{T} : one with essential boundary in $\partial\tilde{T}$, that we shall call *essential preimage* and denote by δ_{ess} ; and the other one inside the interior of \tilde{T} , that we shall call *contractible preimage* and denote by δ_0 . See Figure 10 for a picture. The co-orientation of T induces a cyclic order on the set of essential preimages and hence on C . Moreover, essential preimages cut \tilde{T} into a union of filled cylinders. For each $\delta \in C$, we define $h(\delta)$ as the element of C such that δ_0 belongs to the filled cylinder comprised between $h(\delta)_{\text{ess}}$ and its direct successor. To δ , we also associate $\varepsilon(\delta) \in \{\pm 1\}$ as follows. Let x be any point in the interior of δ , x_{ess} its preimage in δ_{ess} and x_0 its preimage in δ_0 . Let (u, v, w) be the image in $T_x S^4$ of a positive basis for $T_{x_0} \tilde{T}$ and z the image in $T_x S^4$ of a normal vector for δ_{ess} at x_{ess} which is positive according to the co-orientation of T . Then (u, v, w, z) is a basis of $T_x S^4$ and we set $\varepsilon(\delta) := 1$ if it is a positive basis and $\varepsilon(\delta) := -1$ otherwise. See Figure 10 for a picture. We define $W(T)$ to be the welded torus corresponding to the welded Gauss diagram $G : C \rightarrow \{\pm 1\} \times G$ defined by $G(\delta) = (\varepsilon(\delta), h(\delta))$.

Proposition 2.4. *The map $T : w\mathcal{T} \rightarrow r\mathcal{T}$ is a bijection.*

Proof. It is straightforwardly checked that $W \circ T = \text{Id}_{w\mathcal{T}}$. It is hence sufficient to prove that either T is surjective or W is injective. It follows from the work of Yanagawa in [Yan69] and Kanenobu–Shima in [KS02] that T is surjective. More detailed references can be found in the proof of Lemmata 2.12 and 2.13 of [ABMW14]. Nevertheless, we shall sketch here an alternative proof which only uses a much less involved result — namely, that flatly embedded 3–balls in B^4 can be put in a position so they project onto embedded 3–balls in B^3 — and shows instead that W is injective.

Let T_1 and T_2 be two ribbon tori such that $W(T_1) = W(T_2)$. There is hence a bijection $\psi : C_1 \rightarrow C_2$, where C_i is the set of ribbon disks of T_i , which preserves the cyclic orders induced by the co-orientations. We consider \tilde{T}_1 and \tilde{T}_2 the abstract solid tori of T_1 and T_2 . Let $\delta \in C_1$, we extend $\delta_0 \subset \tilde{T}_1$ into a disk δ'_0 which is disjoint from the other disk extensions and from the essential preimages, and whose boundary is an essential curve in $\partial\tilde{T}_1$. Moreover, the co-orientation of T_1 on δ_{ess} and δ'_0 provide two normal vectors for δ . We choose δ'_0 so that, up to isotopy, these vectors coincide. Note that, in doing such an extension of contractible preimages, we fix an arbitrary order on the contractible preimages which are in the same filled cylinder; and, more globally, a cyclic order on the union of essential and contractible preimages. Now, for every ribbon disk $\delta \in C_1$, we consider a small neighborhood $V(\delta)$ of the image of δ'_0 in S^4 . Locally, it looks like in Figure 3 and $V(\delta) \cap T_1$ is the union of four disks that we shall call the *ribbon disk ends* of δ . By considering a tubular neighborhood of a path which visits each $V(\delta)$ successively but avoids T_1 otherwise, we extend $\bigsqcup_{\delta \in C_1} V(\delta)$ into a 4–ball $B_* \subset S^4$ which meets T_1 only in $\bigsqcup_{\delta \in C_1} V(\delta)$.

Similarly, we extend the contractible preimages of T_2 in such a way that the global cyclic order on all preimages corresponds, *via* ψ , to the one of T_1 — this is possible only under the assumption that $W(T_1) = W(T_2)$ — and we perform an isotopy on T_2 so $T_2 \cap B_* = T_1 \cap B_*$ with ribbon disks identified *via* ψ . In particular, ribbon disk ends of T_1 and T_2 coincide. Outside B_* , T_1 and T_2 are now both disjoint unions of embedded 3–balls which associate pairwise all the ribbon disk ends in the same way. We put them in a position in $B_C := S^4 \setminus \mathring{B}_* \cong B^4$ so that they project onto disjoint embedded 3–balls in B^3 . The fact that each 3–ball is twice attached by disks to ∂B_* may introduce several wens, but since all ribbon disk ends can be oriented coherently using the co-orientation, for instance, of T_1 , there are an even number of them on each component and, as we shall see in the next section, they cancel pairwise. The projections are then the tubular neighborhoods of two string links in B^3 on which the local isotopy shown in Figure 13 allows us to perform crossing changes. It follows that $T_2 \cap B_C$ can be transformed into $T_1 \cap B_C$, so $T_1 = T_2$ in $r\mathcal{T}$. The map W is then injective. \square

Welded tori are then a faithful combinatorial description of ribbon tori. Since a contraction-to-the-core inverse shows easily that the map $B : w\mathcal{T} \rightarrow b\mathcal{T}$ is surjective, broken tori are also in one-to-one correspondence with ribbon and welded tori.

Proposition 2.5. *The map T descends to a well-defined surjective map $\text{Tube} : w\mathcal{K} \rightarrow r\mathcal{K}$.*

Proof. It is sufficient to prove that any two broken tori which differ by a broken Reidemeister move only are sent through T to ribbon tori which can be realized with same boundary (but different fillings). This is done in Figure 14, 15, 16 and 17. There, the upper lines give 4–dimensional movies of filled tubes which project along the height axis —time becomes then the new height parameter— to the pieces of broken torus diagram shown on Figure 4 as the left hand sides of the broken moves; and the lower lines give another fillings of the very same tubes, which, after a suitable deformation, project along the height axis to the right hand sides of the same broken moves. Movies are hence read from left to right, one line out of two. For instance, line 1 continues on line 3. For Reidemeister moves II and III, we have dropped the left–right motion of the disks since it plays no role, complicates uselessly the pictures and can be easily added in the reader’s mind.

Surjectivity is immediate by Proposition 2.4. \square

Now, we can address the question of the Tube map injectivity. It is directly checked that classical Reidemeister moves on welded tori are in one-to-one correspondance with broken Reidemeister moves on broken tori. It follows that the notions of welded and broken knots do coincide. So, basically, it remains to understand whether Reidemeister moves on broken tori are sufficient to span the whole ∂ –equivalence relation on $r\mathcal{T}$. As noticed in [Win09], the answer is no. Indeed, since it forgets everything about the filling, the

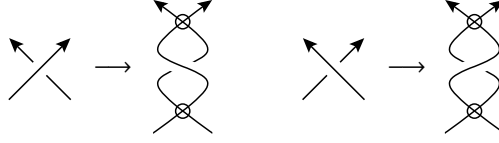


FIGURE 11. Signs reversal on virtual diagrams

∂ -equivalence is insensitive to a change of co-orientation. However, as noted in Remark 2.1, it is not sufficient to reverse the orientation of a welded torus for its image under B to be identical but with reversed co-orientation: one also need to reverse all the crossing signs and add virtual crossings on both sides of each classical crossing.

Notation 2.6. For any virtual diagram D , we define $-D$ to be the virtual diagram obtained by reversing the orientation of D and by \bar{D} the diagram obtained by applying to each classical crossing of D the operation described in Figure 11. These operations on \mathbf{vD} factor through the quotients \mathbf{wT} and \mathbf{wK} . From the welded Gauss diagram point of view, the second is nothing but to the reversal of all signs.

We define a *global reversal* as the simultaneous reversing of both the orientation and the signs; it is denoted by glRev in Figure 2.

It follows from the discussion above that:

Proposition 2.7. *The Tube map is invariant under global reversal, that is $\text{Tube}(K) = \text{Tube}(-\bar{K})$ for every welded knot K .*

3. A DIGRESSION ON WENS

In this section, we focus on a particular portion of ribbon torus-knot, called wen in the literature. A detailed treatment of them can be found in [KS02], [BND14a, Sec. 2.5.4] and [BND14b, Sec. 4.5]. In general, a wen is an embedded Klein bottle cut along a meridional circle. Locally, it can be described as a circle which makes a half-turn inside a 3-ball with an extra time parameter.

Definition 3.1. A *wen* is an embedded annulus in S^4 which can be locally parametrized as

$$(\gamma_t(C), t)_{t \in [0,1]} \subset B^3 \times [0, 1] \subset S^4$$

where $C \subset B^3$ is a fixed circle and $(\gamma_t)_{t \in [0,1]}$ a path in $\text{Diff}(B^3; \partial B^3)$, the set of smooth diffeomorphisms of B^3 which fix the boundary, such that γ_0 is the identity and γ_1 a diffeomorphism which sends C on itself but with reversed orientation.

A wen by itself is rather pointless since the reparametrization $\varphi(x, y, z, t) := (\gamma_t^{-1}(x, y, z), t)$ sends it on a trivially embedded annuli and, reciprocally, any annuli can be reparametrized as a wen. However, as a portion of a ribbon torus-knots, we shall be interested in modifying a wen without altering the rest of the ribbon torus-knot. In this prospect, we shall consider only isotopies of S^4 which fix the boundary components of wens. We shall say then that the wens are ∂ -isotopic.

Generically, a wen projects in B^3 into one of the four pieces of non symmetric broken torus diagram shown in Figure 12. However, we can speak of a wen unambiguously since the following result holds:

Proposition 3.2. [KS02, Lem. 3.1] *Any two wens are ∂ -isotopic in S^4 .*

It has the following corollary, depicted in the last four pictures of Figure 18:

Corollary 3.3. *The gluing of any two wens along one of their boundary circles is ∂ -isotopic to a trivially embedded cylinder.*

Although it is a direct consequence of T. Kanenobu and A. Shima's result, we shall sketch an alternative proof which strongly relies on the Smale conjecture proved by A. Hatcher in [Hat83].

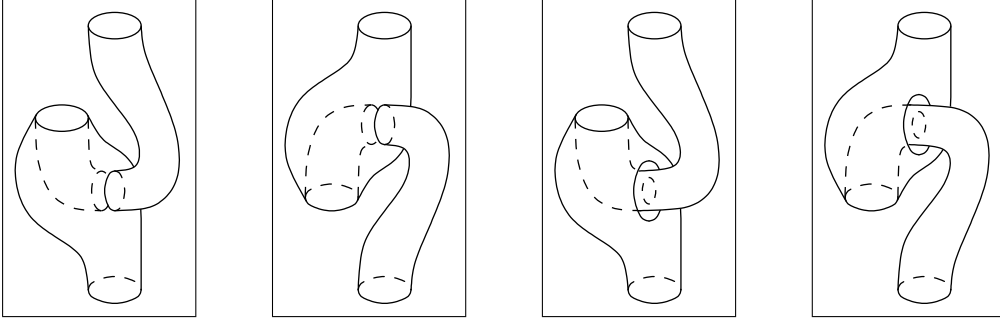


FIGURE 12. The four projections of wens

Proof. We consider two paths $(\gamma_t^1)_{t \in [0,1]}$ and $(\gamma_t^2)_{t \in [0,1]}$ in $\text{Diff}(B^3; \partial B^3)$ which parametrizes, respectively, the first and the second wens. By composing the second path with γ_1^1 and gluing it to the first one, we obtain a parametrization of the two wens as $(\gamma_t^0(C), t)_{t \in [0,1]}$ where γ^0 is a path in $\text{Diff}(B^3; \partial B^3)$ which starts at the identity and ends at $\gamma_1^2 \circ \gamma_1^1$ which is a smooth diffeomorphism of B^3 sending C to itself with same orientation.

To define an ambient isotopy of S^4 , it would be more convenient that γ^0 also ends at the identity. This can be achieved by slightly packing down the two wens from the top, and reparametrizing the small piece of trivially embedded annulus that it creates. In this prospect, we define now a path $(\gamma_t)_{t \in [0,1]}$ of elements in $\text{Diff}(B^3; \partial B^3)$ which starts at $\gamma_1^0 = \gamma_1^2 \circ \gamma_1^1$, ends at the identity and preserves globally C for each $t \in [0, 1]$. Since the set $\text{Diff}^+(S^1)$ of orientation preserving smooth diffeomorphisms of S^1 is path connected, there is a path between the restriction of γ_1^0 to C and the identity on C . It can be used to deform γ_1^0 in a neighborhood of C into a diffeomorphism $\gamma_{\frac{1}{3}}$ which fixes both ∂B^3 and C . Then, we choose an arbitrary path λ from a point of C to a point of ∂B^3 . Possibly up to an infinitesimal deformation of $\gamma_{\frac{1}{3}}$, we may assume that λ and $\gamma_{\frac{1}{3}}(\lambda)$ meet only at their extremities, so $\lambda \cup \gamma_{\frac{1}{3}}(\lambda)$ is a closed curve embedded in B^3 . Let D be any disk in B^3 bounded by this curve. The diffeomorphism $\gamma_{\frac{1}{3}}$ can now be deformed in a neighborhood of D so the image of λ is pushed along D to λ . It results a diffeomorphism which fixes ∂B^3 , C and λ . We can deform it furthermore so we obtain a diffeomorphism $\gamma_{\frac{2}{3}}$ which fixes a tubular neighborhood N of $C \cup \lambda \cup \partial B^3$. But $S^3 \setminus N$ is a solid torus — gluing another 3–ball B to B^3 gives a 3–sphere, and the union of B with N is an unknotted torus whose complement in the 3–sphere is also a torus — and since $\text{Diff}(S^1 \times D^2; \partial S^1 \times D^2)$ is contractible, see formulation (9) of the Smale conjecture in [Hat83, Appendix], there is path from $\gamma_{\frac{2}{3}}$ to the identity.

After being packed down, the two wens are now reparametrized as $(\gamma_{\frac{t}{1-\varepsilon}}^0(C), t)_{t \in [0, 1-\varepsilon]} \cup (\gamma_{\frac{t-1+\varepsilon}{\varepsilon}}^0(C), t)_{t \in [1-\varepsilon, 1]}$, for some small $\varepsilon > 0$. This defines a loop of smooth diffeomorphisms of B^3 which fixes ∂B^3 . But since $\text{Diff}(B^3; \partial B^3)$ is contractible, see formulation (1) of the Smale conjecture in [Hat83, Appendix], it is homotopic to the trivial loop. This provides an homotopy of $B^3 \times [0, 1] \subset S^4$ which deforms the two glued wens into a trivially embedded annulus. Since it fixes the boundary of $B^3 \times [0, 1]$, it can be extended by identity to an homotopy of S^4 . \square

Now we enumerate three consequences of Corollary 3.3.

Untwisting twisted 3–balls: Wens are no obstruction for a torus in S^4 to admit a ribbon filling. Indeed, one can similarly flip disks instead of circles, and all the arguments above apply to wens filled in this way. This is used in the proof of Proposition 2.4: when rectifying 3–balls so they project properly in B^3 , some twisting may arise near the fixed ribbon disk ends. This can be untwisted using filled wens, and those cancel pairwise thanks to the filled version of Corollary 3.3.

Reidemeister I move for ribbon surfaces: Since it cannot be interpreted in terms of flying rings, it may be worthwhile to pay more attention to move RI on broken torus diagrams. So, besides its realization as a change of filling given in Figure 14 and 15, we provide in Figure 18 an isotopy in S^4 , seen from the (non symmetric) broken torus diagram point of view, which realizes a move RI with the help of Proposition 3.2. The left handside of move RI in Figure 4 can indeed be seen to be

isotopic to the last picture in Figure 18 by pulling one singular circle next to the other. Note that the last five pictures can be replaced by a single use of Corollary 3.3.

Commutation of the Tube map with the orientation reversals: A consequence of Corollary 3.3 is that a trivially embedded torus can be inverted in S^4 . Indeed, one can choose any portion of the torus and create *ex nihilo* a pair of wens. Then, one of the wens can travel all along the torus, inverting on its way the orientation. Once done, wens can cancel back one each other.¹

The same isotopy can be performed even if the torus is knotted, but then the passage of the wen will modify the neighborhood of each ribbon disk. Indeed, as explained in [BND14b, Sec. 4.5], it will reverse the sign associated to each ribbon disk. Starting with $\text{Tube}(K)$, for K any welded knot, the isotopy will hence end at $-\text{Tube}(\overline{K})$. The torus inversion process in S^4 induces then the following:

Proposition 3.4. *For every welded knot K , $\text{Tube}(K) = -\text{Tube}(\overline{K})$.*

Together with Proposition 2.7, it implies:

Proposition 3.5. *For every welded knot K , $\text{Tube}(-K) = \text{Tube}(\overline{K}) = -\text{Tube}(K)$.*

Question 3.6. Is there a one-to-one correspondence between ribbon torus-knots and welded knots up to global reversal? Equivalently, do the classical Reidemeister local moves and the co-orientation reversal generate all possible change of filling?

REFERENCES

- [ABMW14] B. Audoux, P. Bellingeri, J.B. Meilhan, and E. Wagner, *Homotopy classification of ribbon tubes and welded string links*, preprint, 2014.
- [Art25] Emil Artin, *Zur Isotopie zweidimensionaler Flächen im \mathbb{R}_4* , Abh. Math. Semin. Univ. Hamb. **4** (1925), 174–177 (German).
- [BB14] Valeriy G. Bardakov and Paolo Bellingeri, *Groups of virtual and welded links*, J. Knot Theory Ramifications **23** (2014), no. 3, 23.
- [BND14a] D. Bar-Natan and Z. Dancso, *Finite type invariants of w-knotted objects I: w-knots and the Alexander polynomial*, arXiv e-prints:1405.1956, 2014.
- [BND14b] ———, *Finite type invariants of w-knotted objects II: Tangles, foams and the Kashiwara-Vergne problem*, arXiv e-prints:1405.1955, 2014.
- [BT99] A. Bartels and P. Teichner, *All two dimensions links are null homotopic*, Geom. Topol. **3** (1999), 235–252 (English).
- [CKS02] J.Scott Carter, Seiichi Kamada, and Masahico Saito, *Stable equivalence of knots on surfaces and virtual knot cobordisms*, J. Knot Theory Ramifications **11** (2002), no. 3, 311–322 (English).
- [Coc83] T. Cochran, *Ribbon knots in S^4* , J. Lond. Math. Soc., II. Ser. **28** (1983), 563–576 (English).
- [Dal14] E. Dalvit, *Rings movie for a virtual crossing*, available at <http://science.unitn.it/~dalvit/visualization/virtualcrossingrings/>, 2014.
- [Fie01] T Fiedler, *Gauss diagram invariants for knots and links*, Mathematics and its Applications, vol. 532, Kluwer Academic Publishers, Dordrecht, 2001.
- [FM66] R.H. Fox and John W. Milnor, *Singularities of 2-spheres in 4-space and cobordism of knots*, Osaka J. Math. **3** (1966), 257–267 (English).
- [FRR97] Roger Fenn, Richárd Rimányi, and Colin Rourke, *The braid-permutation group*, Topology **36** (1997), no. 1, 123–135.
- [GPV00] M. Goussarov, M. Polyak, and O. Viro, *Finite type invariants of virtual and classical knots*, Topology **39** (2000), 1045–1168.
- [Hat83] Allen E. Hatcher, *A proof of the Smale conjecture*, $\text{Diff}(S^3) \simeq \text{O}(4)$, Ann. of Math. (2) **117** (1983), no. 3, 553–607.
- [IK12] Atsushi Ichimori and Taizo Kanenobu, *Ribbon torus knots presented by virtual knots with up to four crossings*, Journal of Knot Theory and Its Ramifications **21** (2012), no. 13, 1240005.
- [Ker65] Michel A. Kervaire, *Les nœuds de dimensions supérieures*, Bull. Soc. Math. Fr. **93** (1965), 225–271 (French).
- [Kim00] Se-Goo Kim, *Virtual knot groups and their peripheral structure*, J. Knot Theory Ramifications **9** (2000), no. 6, 797–812.
- [KM61] M.A. Kervaire and John W. Milnor, *On 2-spheres in 4-manifolds*, Proc. Natl. Acad. Sci. USA **47** (1961), 1651–1657 (English).
- [KS02] T. Kanenobu and A. Shima, *Two filtrations of ribbon 2-knots*, Proceedings of the First Joint Japan-Mexico Meeting in Topology (Morelia, 1999), vol. 121, 2002, pp. 143–168.
- [Kup03] Greg Kuperberg, *What is a virtual link?*, Algebr. Geom. Topol. **3** (2003), 587–591.
- [PV94] M. Polyak and O. Viro, *Gauss diagram formulas for Vassiliev invariants*, Internat. Math. Res. Notices (1994), no. 11, 445ff., approx. 8 pp. (electronic).
- [Sat00] S. Satoh, *Virtual knot presentation of ribbon torus-knots*, J. Knot Theory Ramifications **9** (2000), no. 4, 531–542.

¹An illustration can be found at <https://www.youtube.com/watch?v=kQcy5Dvpv1M>

- [Suz76] Shin'ichi Suzuki, *Knotting problems of 2-spheres in 4-sphere.*, Mathematics Seminar Notes Vol. 4, No.3, 241-371. Kobe, Japan: Kobe University. (1976)., 1976.
- [SW00] Daniel S. Silver and Daniel S. Williams, *Virtual knot groups.*, Knots in Hellas '98. Proceedings of the international conference on knot theory an its ramifications, European Cultural Centre of Delphi, Greece, August 7–15, 1998, Singapore: World Scientific, 2000, pp. 440–451.
- [Win09] B. Winter, *The classification of spun torus knots.*, J. Knot Theory Ramifications **18** (2009), no. 9, 1287–1298 (English).
- [Yaj62] Takeshi Yajima, *On the fundamental groups of knotted 2-manifolds in the 4-space*, J. Math. Osaka City Univ. **13** (1962), 63–71. MR 0151960 (27 #1941)
- [Yaj64] T. Yajima, *On simply knotted spheres in \mathbb{R}^4* , Osaka J. Math. **1** (1964), 133–152.
- [Yan69] T. Yanagawa, *On ribbon 2-knot. The 3-manifold bounded by the 2-knots*, Osaka J. Math. **6** (1969), 447–464.

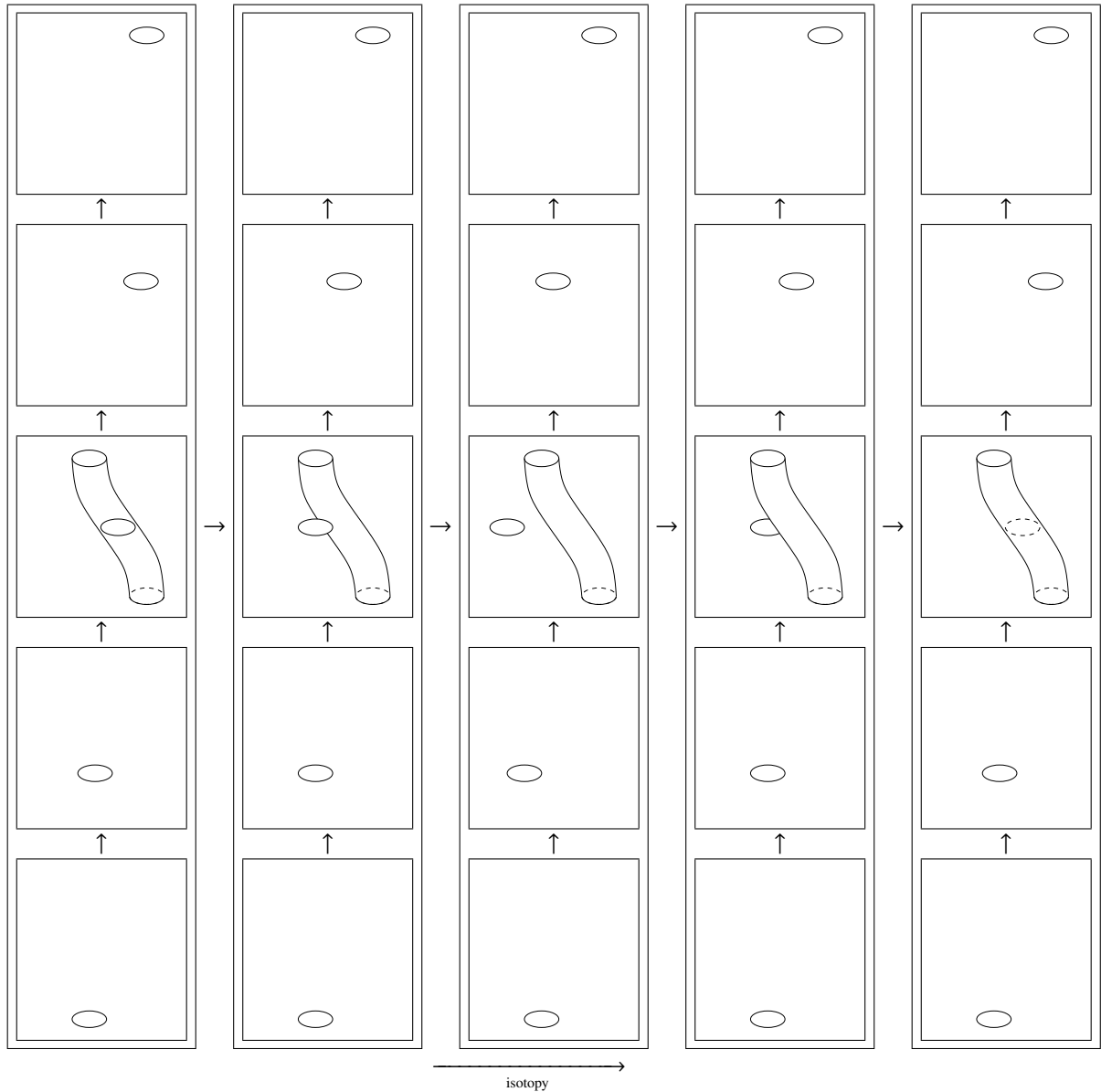


FIGURE 13. Isotopy for the virtual move

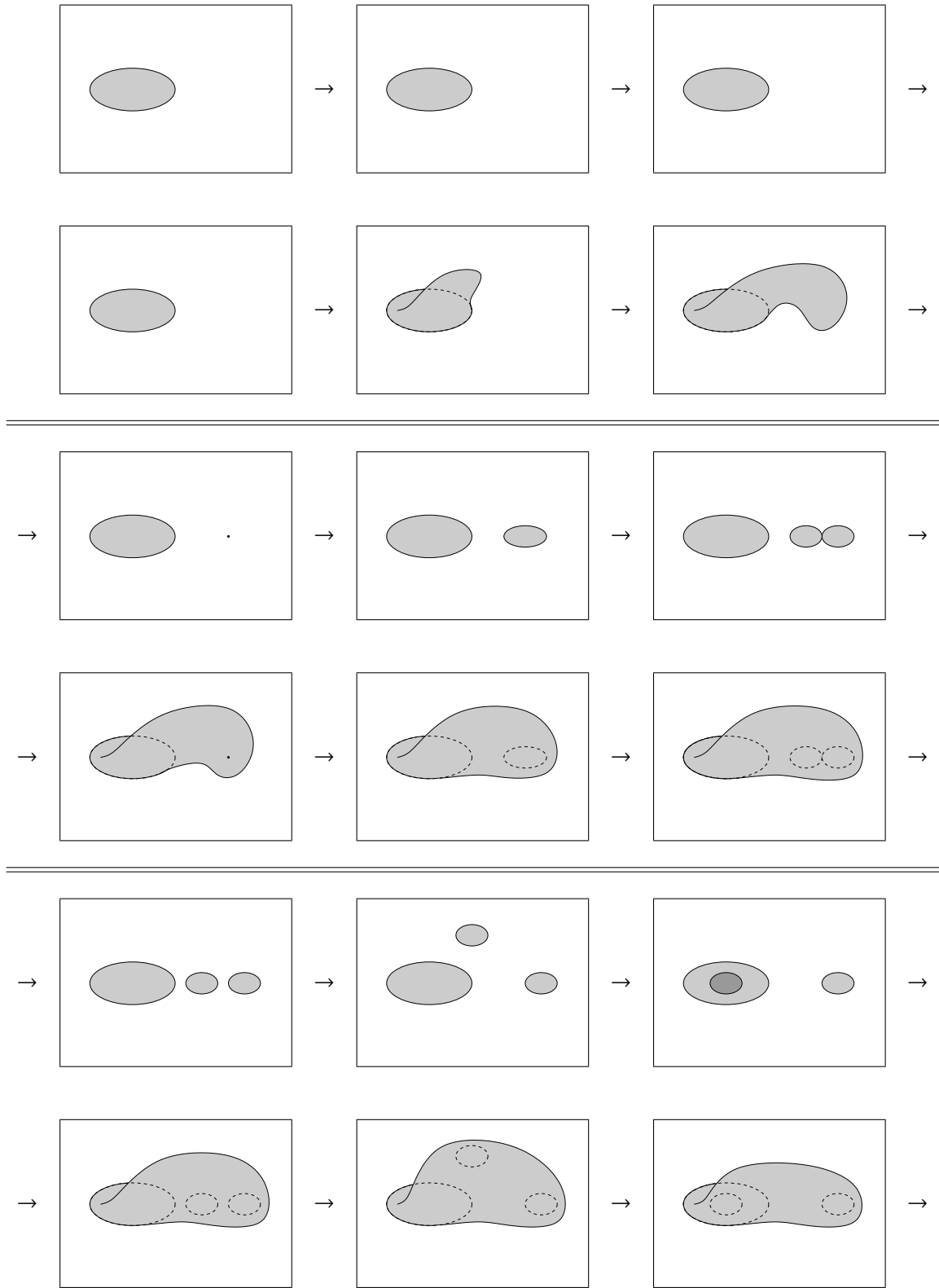


FIGURE 14. RI seen as a filling change (part 1)

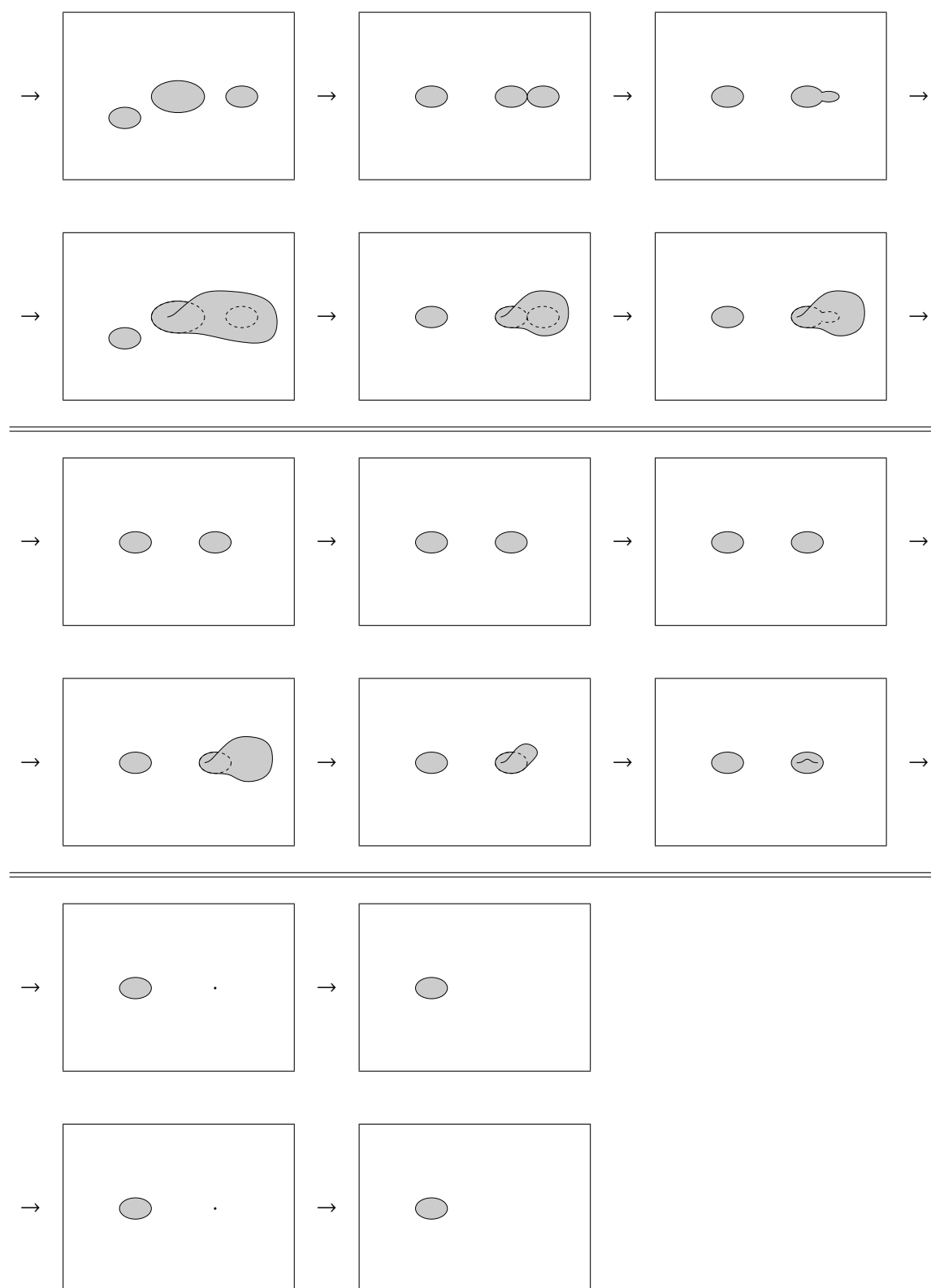


FIGURE 15. RI seen as a filling change (part 2)

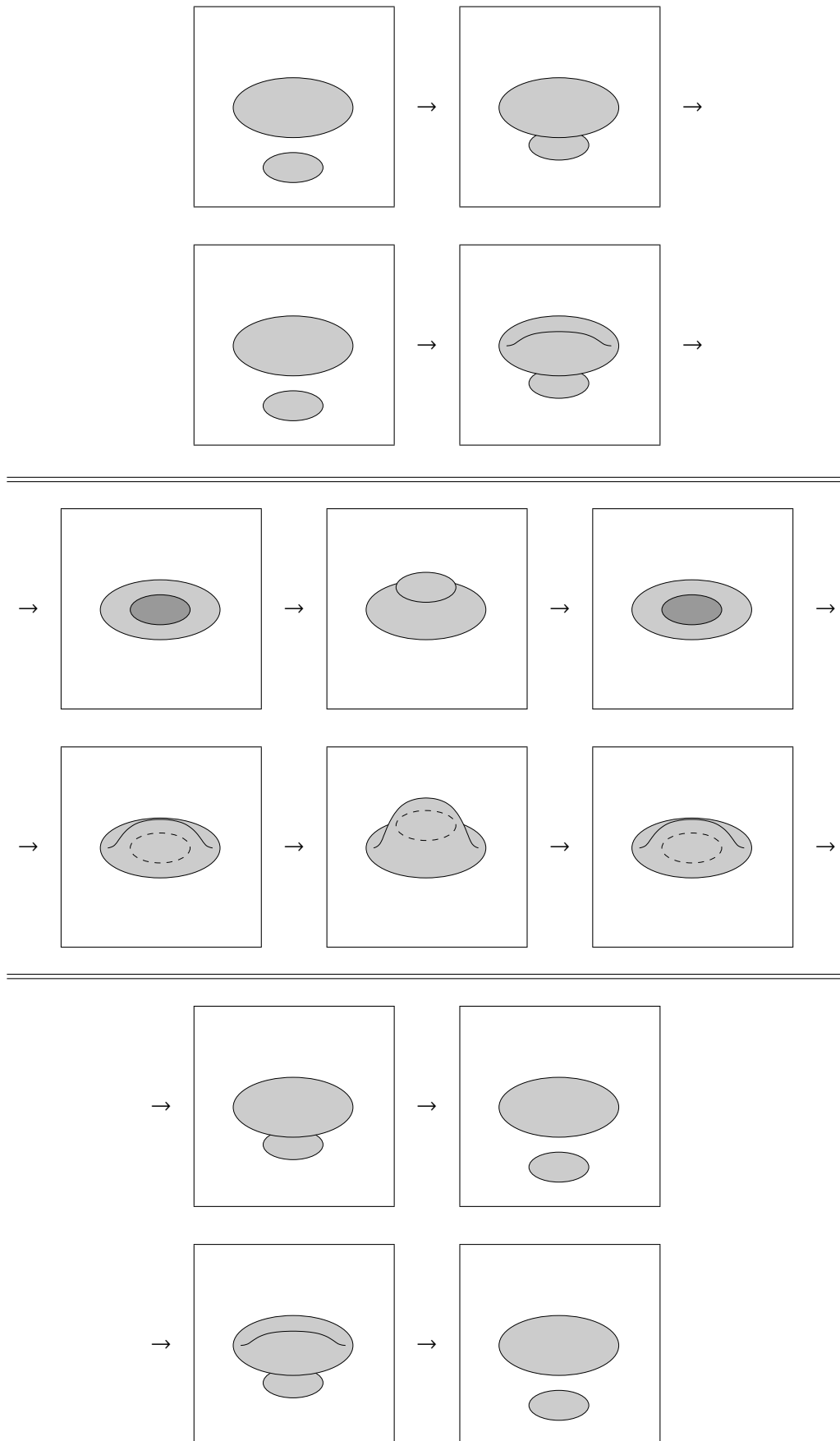


FIGURE 16. RII seen as a filling change

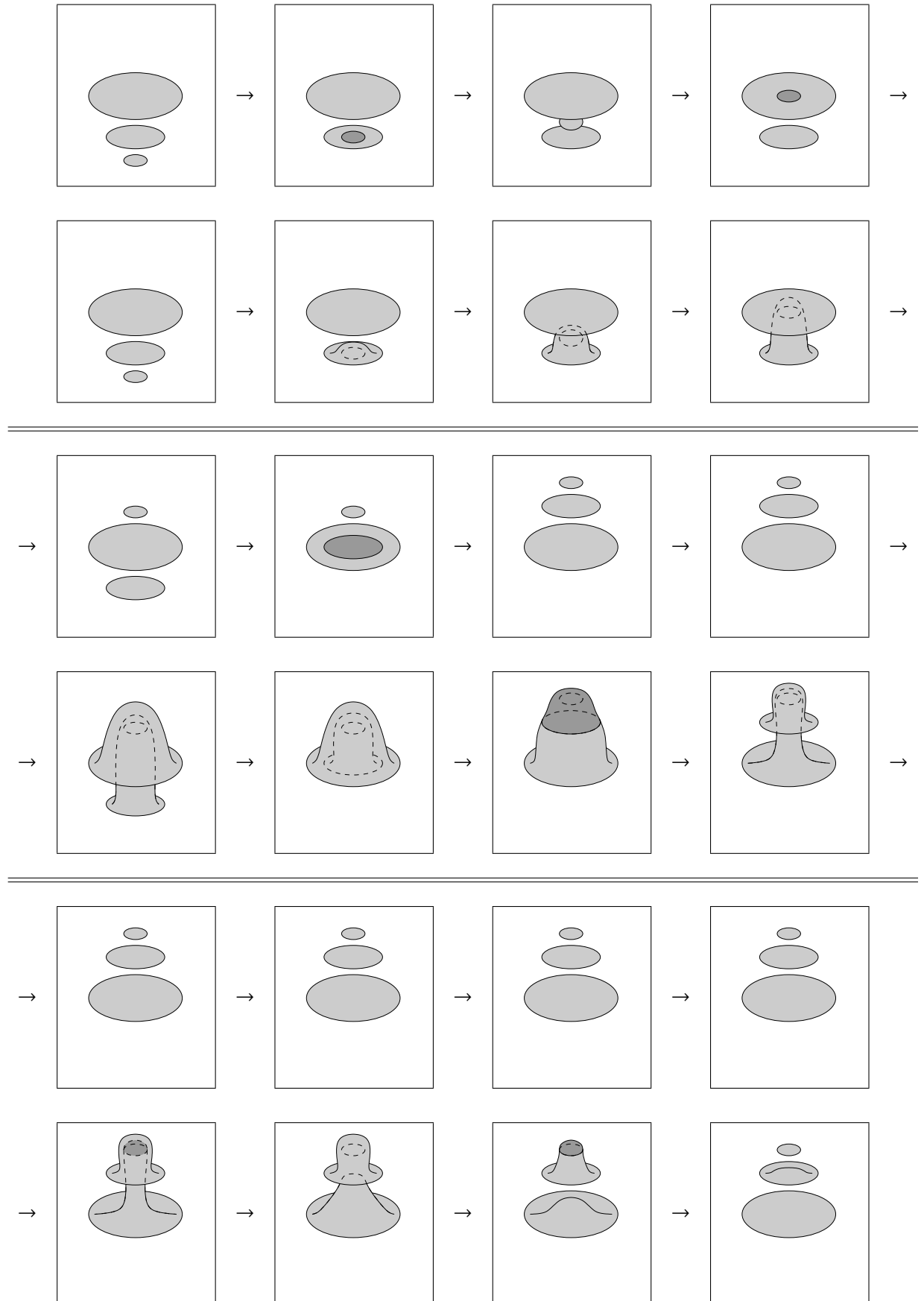


FIGURE 17. RIII seen as a filling change

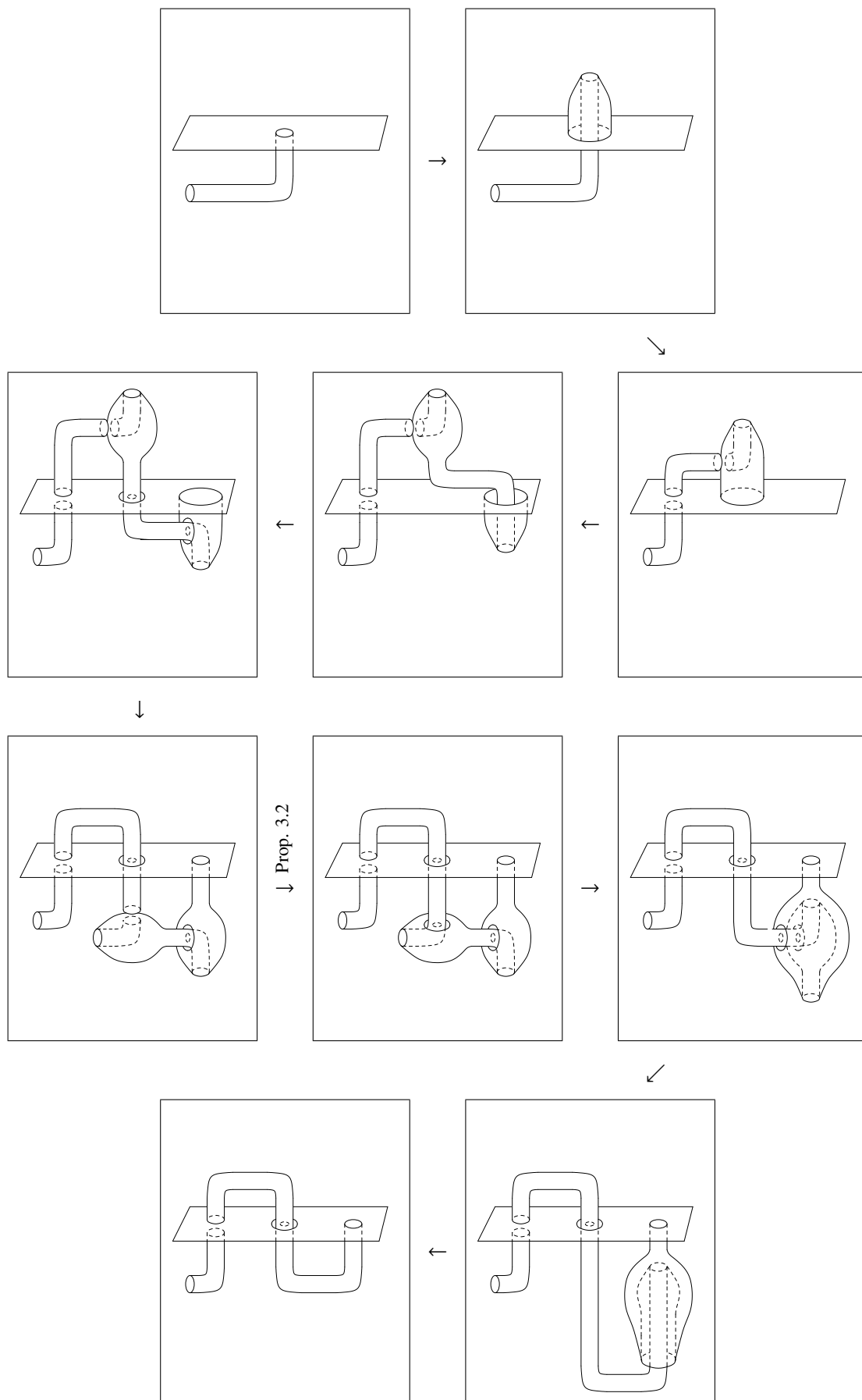


FIGURE 18. RI seen as a wen cancellation